

Chiral symmetry breaking, instantons, and monopoles

Adriano Di Giacomo

University of Pisa, Department of Physics and INFN, Sezione di Pisa, Largo B. Pontecorvo 3, 56127, Pisa, Italy

E-mail: digiacco@df.unipi.it

Masayasu Hasegawa*

Joint Institute for Nuclear Research, Bogoliubov Laboratory of Theoretical Physics, Dubna, 141980, Moscow, Russia

E-mail: hasegawa@theor.jinr.ru

The purpose of this study is to show that monopoles induce the chiral symmetry breaking. In order to indicate the evidence, we add one pair of monopoles with magnetic charges to the quenched SU(3) configurations by a monopole creation operator, and investigate the properties of the chiral symmetry breaking using the Overlap fermion. We show that instantons are created by the monopoles. The pseudoscalar meson mass and decay constant are computed from the correlation functions, and the renormalization constant Z_S is determined by the non perturbative method. The renormalization group invariant chiral condensate in $\overline{\text{MS}}$ -scheme at 2 [GeV] is evaluated by the Gell-Mann-Oakes-Renner formula, and the random matrix theory. Finally, we estimate the renormalization group invariant quark masses $\bar{m} = (m_u + m_d)/2$, and m_s in $\overline{\text{MS}}$ -scheme at 2 [GeV]. The preliminary results indicate that the chiral condensate decreases and the quark masses become slightly heavy by increasing the number of monopole charges.

The 33rd International Symposium on Lattice Field Theory

14 -18 July 2015

Kobe International Conference Center, Kobe, Japan

*Speaker.

1. Introduction

The quark confinement is caused by the monopole condensation in QCD, that is beautifully explained from the dual superconductivity by t'Hooft and Mandelstams [1]. The instanton configurations induce the chiral symmetry breaking [2, 3]. In this study we want to show that monopoles are related with the instantons and the chiral symmetry breaking, by using the Overlap fermion which preserves the chiral symmetry in the lattice gauge theory [4]. In order to show the relation, we add monopoles with magnetic charges to SU(3) quenched configurations by the monopole creation operator [5]. We compute the low-lying eigenvalues and eigenvectors from the gauge links of normal configurations and configurations with additional monopoles, by solving eigenvalue problems of the Overlap Dirac operator [6, 7].

In previous work we have shown that the topological susceptibility in the continuum limit is properly computed, and the instanton density is consistent with the values computed from instanton liquid model in Ref. [2]. The additional monopoles form long loops in QCD vacuum. Instantons are created by the additional monopoles, moreover, the additional monopoles do not affect detection of the fermion zero modes [8]. Our study in the Maximal Abelian gauge shows that the number of observed zero modes increases with the square root of the total physical length of monopole loops, and the number of instantons is in direct proportion to the total physical length of monopole loops [9]. Moreover, in the study of the random matrix theory, we have precisely computed the chiral condensate which is the order parameter of the chiral symmetry breaking. We have confirmed that the additional monopoles do not affect the low-lying eigenvalues of the Overlap Dirac operator, and found that the chiral condensate decreases by increasing the magnetic charges of the additional monopoles [10]. This is an evidence that monopoles directly induce the chiral symmetry breaking.

However, those studies have been done by adding monopoles with charges to the small lattice volume ($V = 14^4$) and one lattice spacing ($\beta = 6.00$). Therefore, we have to investigate the values at the continuum limit and the finite lattice volume effects. In present study we add monopoles with magnetic charges to configurations of the larger lattices volumes and different parameters of lattice spacing.

In this report, we count the number of instantons from the average squares of the topological charges, and compute the instanton density from the normal configurations. We show that one instantons of \pm charge is created by one pair of monopoles with magnetic charges $m_c = \pm 1$ [Section 2]. Next, we compute the pseudoscalar meson mass and decay constant from the correlation functions, and derive the renormalization constant Z_S by the non perturbative method. The renormalization group invariant chiral condensate in the $\overline{\text{MS}}$ -scheme at 2 [GeV] is evaluated by the Gell-Mann-Oakes-Renner (GMOR) formula, and the random matrix theory (RMT). The results of the chiral condensate which are computed from normal configurations are $\langle \bar{\psi}\psi \rangle_{\overline{\text{MS}}}^{\text{GMOR}}(2 \text{ GeV}) = -0.0271(13) [\text{GeV}^3]$, $\langle \bar{\psi}\psi \rangle_{\overline{\text{MS}}}^{\text{RMT}}(2 \text{ GeV}) = -0.0269(14) [\text{GeV}^3]$, ($r_0 = 0.5[\text{fm}]$). The renormalization group invariant quark masses, $\bar{m} = (m_u + m_d)/2$ and m_s , in the $\overline{\text{MS}}$ -scheme at 2 [GeV] are estimated. The results which are computed for normal configurations are $\bar{m}^{\overline{\text{MS}}}(2 \text{ GeV}) = 4.0(4) [\text{MeV}]$, and $m_s^{\overline{\text{MS}}}(2 \text{ GeV}) = 98(9) [\text{MeV}]$, ($a^{-1} = 2.00(8) [\text{GeV}]$).

Lastly, the preliminary results show that the chiral condensate decreases with increasing the number of monopole charges. The quark masses become slightly heavy with increasing the number of monopole charges [Section 3].

2. Instantons and monopoles

2.1 Overlap fermions

The Overlap fermion preserves the chiral symmetry in the lattice gauge theory, and has the fermion zero modes [4]. The massless Overlap Dirac operator is computed from the massless Wilson Dirac operator, which is constructed from the gauge links of the configurations [6, 7]. In this study the (negative) mass parameter is $\rho = 1.4$, and the numbers of low-lying eigenvalues and eigenvectors of the Overlap Dirac operator are $\mathcal{O}(40 - 100)$, which are computed by solving the eigenvalue problems using the subroutines (ARPACK). In this section, the lattice spacing is computed from the interpolating function [11]. The scale is $r_0 = 0.5$ [fm].

Let n_+ be the number of zero modes of chirality plus, n_- the number of those with chirality minus. Those numbers are counted from exact zero modes in spectra of the Overlap Dirac operator. The topological charge is defined as $Q = n_+ - n_-$. The topological susceptibility is computed from $\langle Q^2 \rangle / V$.

However, in our simulation, we never observed the zero modes of chiralities n_+ and n_- in one configuration at the same time. Therefore, to check the reason, we compare the distribution of the topological charges with the results produced by the other group. Moreover, we compute the topological susceptibility at the continuum limit, by interpolating five data points ($\beta = 5.8124, 5.9044, 5.9890, 6.0000, \text{ and } 6.0680$) possessing the same physical volume $V/r_0^4 = 49.96$ to the continuum limit. The fitting function is $\langle Q^2 \rangle r_0^4 / V = c_1 \cdot (a/r_0)^2 + c_0$. The topological susceptibility at the continuum limit in this study is

$$\chi = (194(3) \text{ [MeV]})^4. \quad (2.1)$$

The theoretical prediction is $\chi = (1.80 \times 10^2 \text{ [MeV]})^4$ [12]. The distribution of the topological charges and the value of the topological susceptibility at the continuum limit are consistent with the results in Ref. [13]. Therefore, we can properly compute the topological charges. In our computation, the number of observed zero modes is exactly the same as the topological charge. Accordingly, the observed number of zero modes is the **net** number $n_+ - n_-$.

2.2 Instanton density

The number of instantons N_i is computed from the average square of the topological charges $\langle Q^2 \rangle$. The relation $N_i = \langle Q^2 \rangle$ is analytically derived [8]. Here, we evaluate the instantons density ρ_i from the slope A by fitting a linear function $\langle Q^2 \rangle = A \cdot V/r_0^4 + B$ to 21 data points. The results are

$$\rho_i = 8.0(2) \times 10^{-4} \text{ [GeV}^4\text{]}, B = -0.02(0.10), \chi^2/d.o.f. = 24.4/19.0. \quad (2.2)$$

The intercept B is zero, and $\chi^2/d.o.f.$ is 1.28. The number of instantons is in direct proportion to the physical volume. Our result is exactly consistent with the instanton liquid model $\rho_i = 8 \times 10^{-4} \text{ [GeV}^4\text{]}$ [2].

2.3 Instantons and monopoles

We confirm that we can properly count the number of instantons. We add one pair of a monopole and an anti-monopole varying magnetic charges m_c to configurations, by the monopole

Table 1: The simulation parameters and the fitted results. $A_{Pred.}$ and $B_{Pred.}$ are computed from our prediction. The fitting range FR is m_c unit.

β	a/r_0	V	V/r_0^4	$A_{Pred.}$	$B_{Pred.}$	A	B	FR	$\chi^2/d.o.f.$
5.9256	0.2129	$14^3 \times 28$	157.89	1.0(2)	11.3(6)	1.1(2)	11.6(5)	0 - 4	0.8/3.0
6.0000	0.1863	14^4	46.276	1.00(3)	3.19(7)	1.07(5)	3.07(10)	0 - 4	8.5/3.0
		$14^3 \times 28$	92.553	1.00(14)	6.6(3)	0.94(16)	5.9(3)	0 - 4	43.3/3.0
		$16^3 \times 32$	157.89	1.00(14)	9.1(4)	1.16(17)	10.1(4)	0 - 5	8.5/4.0
6.0522	0.1705	$18^3 \times 32$	157.89	1.00(11)	9.4(4)	1.22(14)	10.6(4)	0 - 6	4.5/5.0

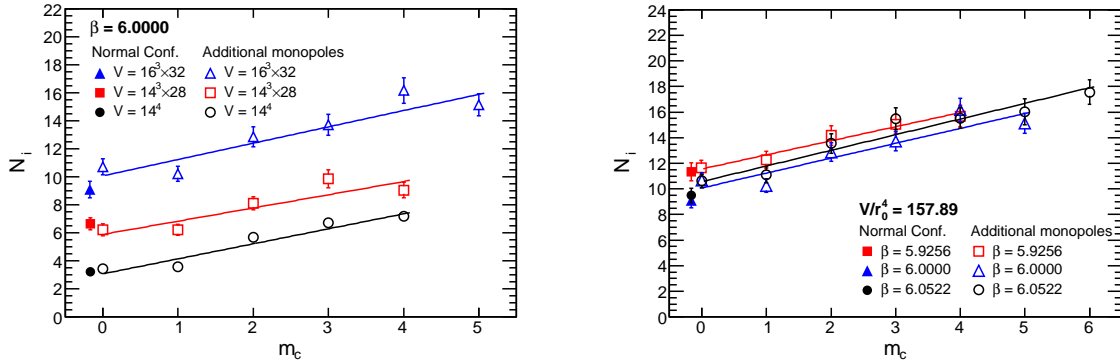


Figure 1: The number of instantons N_i versus the number of monopole charges m_c . The lattice spacing is fixed at $\beta = 6.0000$ (left figure). The physical lattice volume is fixed at $V/r_0^4 = 157.89$ (right figure).

creation operator [5]. The monopole has positive magnetic charges $m_c = +1, +2, \dots, +6$, and the anti-monopole has negative magnetic charges $m_c = -1, -2, \dots, -6$. The total of the magnetic charges in the configuration set to zero. Henceforth, m_c indicates that both charges $\pm m_c$ are added. We put the monopole and the anti-monopole holding the physical distance $D \approx 1.1$ [fm]. We generate configurations setting the lattice spacing at $\beta = 6.0000$ to check the finite lattice volume effects, and setting the physical lattice volume at $V/r_0^4 = 157.89$ to check the continuum limit. The numbers of configurations are $\mathcal{O}(5 \times 10^2) \sim \mathcal{O}(7 \times 10^2)$ for each parameter. The simulation parameters are in Table 1. We fit a linear function $N_i = A \cdot m_c + B$ as show in Fig. 1, and compare the slope A and the intercept B with our prediction in Table 1. The details of our prediction is explained in Ref. [8]. The slope A and the intercept B are consistent with our prediction. The finite lattice volume and the discretization do not affect the results. Therefore, one pair of monopoles with one positive charge and one negative charge creates one instanton of one positive or negative charge.

3. Chiral symmetry breaking and monopoles

We compute the renormalization constant Z_S , and evaluate the renormalization group invariant chiral condensate and quark masses in the $\overline{\text{MS}}$ -scheme at 2 [GeV], using one hundred pairs of low-lying eigenvalues and eigenvectors. The lattice for this study is $V = 16^3 \times 32$, $\beta = 6.0000$. The number of the monopole charges m_c is from zero to five, and the number of configurations N_{conf} is 500 for each measurement.

3.1 The pseudoscalar correlation, renormalization constant, and chiral condensate

In this study the pseudoscalar meson mass m_{PS} is computed from the difference between the pseudoscalar correlation function C_{PP} and the scalar correlation function C_{SS} , $C_{PP-SS} \equiv C_{PP} - C_{SS}$. The correlation functions of the pseudoscalar C_{PP} and the scalar C_{SS} are computed as in Ref. [14]. In order to evaluate precisely the square of pseudoscalar meson mass at the chiral limit, we compute the correlation function C_{PP-SS} at 30 different valence quark masses. The range of the valence quark masses is $0.00472 \leq am_q \leq 0.04721$ ($10 \leq m_q \leq 100$ [MeV]). We determine the the pseudoscalar meson mass m_{PS} and G_{PP-SS} by fitting a following function [15, 16],

$$C_{PP-SS}(t) = \frac{G_{PP-SS}}{am_{PS}} \exp\left(-\frac{am_{PS}T}{2}\right) \cosh\left\{am_{PS}\left(\frac{T}{2}-t\right)\right\}. \quad (3.1)$$

We then compute Z_S as in Refs. [10, 17]. The results are in Table 2. Next, we compute the chiral condensate from Gell-Mann-Oakes-Renner mass formula defined as in Ref. [18],

$$a^3 \langle \bar{\psi}\psi \rangle = - \lim_{am_q \rightarrow 0} \frac{(af_P)^2 (am_{PS})^2}{2(am_q)}, \quad af_P = 2(am_q) \frac{\sqrt{G_{PP-SS}}}{(am_{PS})^2}. \quad (3.2)$$

We convert $\langle \bar{\psi}\psi \rangle$ to the $\overline{\text{MS}}$ -scheme at 2 [GeV] as follows: $\langle \bar{\psi}\psi \rangle^{\overline{\text{MS}}}(2 \text{ GeV}) = \langle \bar{\psi}\psi \rangle Z_S / z$, $z =$

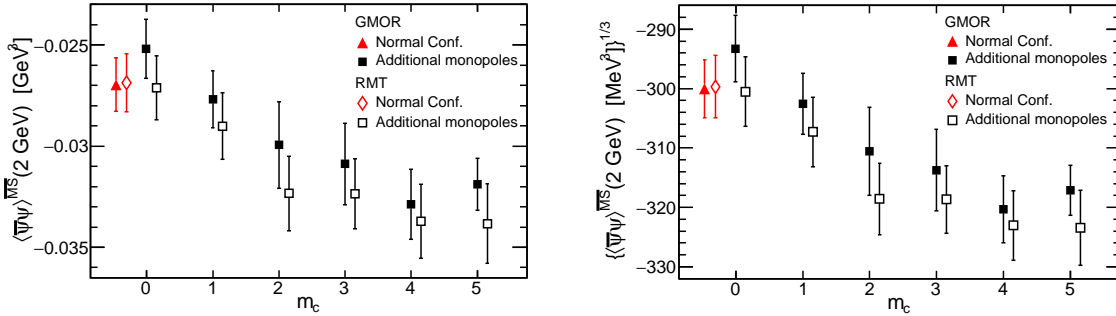


Figure 2: The comparisons of the chiral condensates which are computed from the GMOR formula and the random matrix theory. The left figure is in $[\text{GeV}^3]$ unit, and the right figure is in $[\text{MeV}]$ unit.

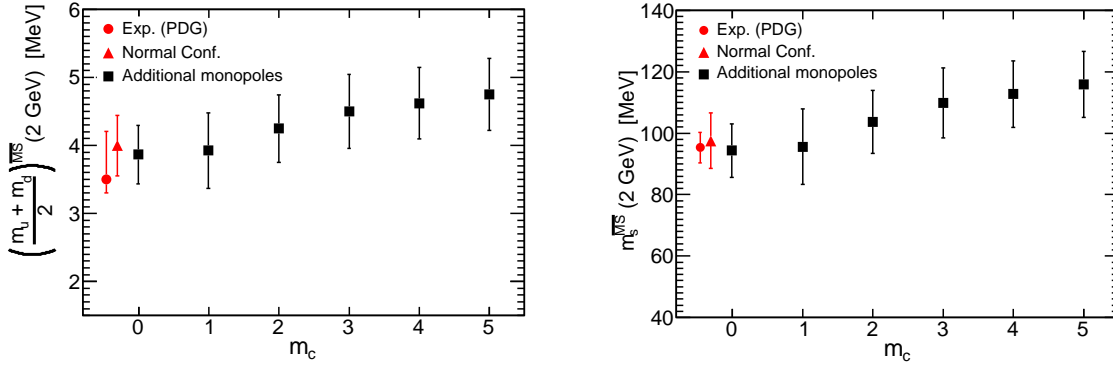
0.72076. The results comparing with the results produced from the random matrix theory are in Table 2. The scale is $r_0 = 0.5$ [fm]. The decay constant at the chiral limit that is computed from normal configurations is $f_\pi = 122.6(1.2)$ [MeV] ($r_0 = 0.5$ [fm]) [16]. The chiral condensates that are computed from GMOR formula and RMT are consistent with each other. The chiral condensate decreases by increasing the monopole charges as shown in Fig 2.

3.2 Quark mass

Lastly, we estimate the quark masses, $\bar{m} = \frac{m_u + m_d}{2}$ and m_s , based on Ref. [16]. The mass ratio is known from the chiral perturbation theory as follows: $R = \frac{m_s}{\bar{m}} = 24.4 \pm 1.5$ [19]. There is a relation between the bare quark mass and the pseudoscalar meson mass following from an assumption of PCAC relation, $m_{PS}^2 = C(m_{q_1} + m_{q_2})$. We determine the coefficient C by fitting a linear function to our data. We then fix the scale a^{-1} for the estimation of the quark masses from a plane of $[(af_P), (am_{PS})^2]$, using the experimental results of the Kaon decay constant $f_{K^-}^{\text{Exp.}} =$

Table 2: The chiral condensates and the quark masses in the \overline{MS} scheme at 2 [GeV]. $\langle\bar{\psi}\psi\rangle^{RMT}$ is computed from the scale parameter Σ in RMT of the topological charge sector $|Q| = 1$. $\bar{m} = (m_u + m_d)/2$.

m_c	Z_S	$\langle\bar{\psi}\psi\rangle_{\overline{MS}}^{GMOR}$ [GeV ³]	$\langle\bar{\psi}\psi\rangle_{\overline{MS}}^{RMT}$ [GeV ³]	$\{\langle\bar{\psi}\psi\rangle_{\overline{MS}}^{GMOR}\}^{1/3}$ [MeV]	$\{\langle\bar{\psi}\psi\rangle_{\overline{MS}}^{RMT}\}^{1/3}$ [MeV]	$\bar{m}^{\overline{MS}}$ [MeV]	$m_s^{\overline{MS}}$ [MeV]
N. C.	0.99(3)	-0.0271(13)	-0.0269(14)	-300(5)	-300(5)	4.0(4)	98(9)
0	1.00(4)	-0.0252(15)	-0.0272(16)	-293(6)	-301(6)	3.9(4)	94(9)
1	1.00(3)	-0.0277(14)	-0.0290(17)	-303(5)	-307(6)	3.9(6)	96(12)
2	0.98(3)	-0.030(2)	-0.0323(18)	-311(7)	-319(6)	4.2(5)	104(10)
3	0.97(3)	-0.031(2)	-0.0324(17)	-314(7)	-319(6)	4.5(5)	110(11)
4	0.98(3)	-0.0329(17)	-0.0337(18)	-320(6)	-323(6)	4.6(5)	113(11)
5	0.99(3)	-0.0319(13)	-0.034(2)	-317(4)	-323(6)	4.8(5)	116(11)

**Figure 3:** The comparisons of the quark masses, $(m_u + m_d)/2$ (left figure) and m_s (right figure) in \overline{MS} -scheme at 2 [GeV]. The experimental results are $\bar{m} = 3.5_{-0.2}^{+0.7}$ [MeV], and $m_s = 95(5)$ [MeV] (PDG).

($156.2 \pm 0.2 \pm 0.6 \pm 0.3$) [MeV] and Kaon mass $m_K^{Exp.} = 493.677 \pm 0.013$ [MeV] (Particle Data Group) as the input values [16, 20]. We do not consider the errors of the experimental results in our computations. The scale that is determined from $f_K(m_K)$ is $a^{-1} = 2.00(8)$ [GeV]. We use this scale to evaluate the quark masses. The quark masses are computed from m_K and the coefficient C as follows: $m_s = \frac{m_K^2}{C(1+\frac{1}{R})}$, $\bar{m} = \frac{m_s}{R}$. Finally, the renormalization group invariant quark mass is estimated as follows: $m^{\overline{MS}} = \hat{Z}_M \cdot m$, $\hat{Z}_M = z/Z_S$, $z = 0.72076$. The results of quark masses are in Table 2. The quark masses that are computed from normal configurations are compatible with the experimental results. The masses slightly become heavy with increasing the monopole charges as shown in Fig. 3.

4. Summary and conclusion

We have confirmed that we properly compute the topological susceptibility and the number of instantons. We have shown that the additional monopoles create instantons. The finite lattice volume and the discretization do not affect the result. The chiral condensate that are computed from the Gell-Mann-Oakes-Renner formula and the random matrix theory are consistent with each other. The quark masses that are computed from normal configurations are consistent with the

experimental results. Lastly, the preliminary results show that the chiral condensate decreases and the quark masses become slightly heavy, by increasing the number of monopole charges.

5. Acknowledgments

The simulations have been performed on, SX-ACE, SX-9, SX-8, and PC clusters at the Research Center for Nuclear Physics and the Cybermedia Center at the University of Osaka, and SR16000 at the Yukawa Institute for Theoretical Physics at the University of Kyoto. We really appreciate their technical supports and the computation time.

References

- [1] G.'tHooft, Nucl. Phys. B **79** (1974) 276; S. Mandelstam, Phys. Rep. **23** (1976) 245.
- [2] E. V. Shuryak, Nucl. Phys. B **203** (1982) 93; Nucl. Phys. B **203** (1982) 116; Nucl. Phys. B **203** (1982) 140.
- [3] D. Diakonov, ArXiv:hep-ph/9602375 (1996).
- [4] P. H. Ginsparg, and K. G. Wilson Phys. Rev. **D 25** (1982) 2649; N. Neuberger, Phys. Lett. B **427** (1998) 353.
- [5] C. Bonati, A. Di Giacomo, and M. D'Elia, Phys. Rev. **D 85** (2012) 065001.
- [6] T. DeGrand (MILC Collaboration), Phys. Rev. **D 63** (2000) 034503.
- [7] L. Giusti, C. Hoelbling, M. Lüscher, and H. Wittig, Comput. Phys. Commun. **153** (2003) 31; L. Giusti, M. Lüscher, P. Weisz, and H. Wittig, JHEP **11** (2003) 023.
- [8] A. Di Giacomo and M. Hasegawa, Phys. Rev. **D 91** (2015) 054512.
- [9] A. Di Giacomo and M. Hasegawa, Cybermedia HPC journal (Osaka University, Japan), No. **5** (2015) 21.
- [10] A. Di Giacomo, M. Hasegawa, and F. Pucci, arXiv:hep-lat/1510.07463 (2015), (PoS (CD15) 127).
- [11] S. Necco, and R. Sommer Nucl. Phys. B **622** (2002) 328.
- [12] E. Witten, Nucl. Phys. B **156** (1979) 269; G. Veneziano, Nucl. Phys. B **159** (1979) 213.
- [13] L. Del Debbio, and C. Pica, JHEP **02** (2004) 003; L. Del Debbio, L. Giusti, and C. Pica, Phys. Rev. Lett. **94** (2005) 032003.
- [14] T. DeGrand and A. Hasenfratz, Phys. Rev. **D 64** (2001) 034512; T. DeGrand and S. Schaefer, Comp. Phys. Commun. **159** (2004) 185.
- [15] V. Giménez, L. Giusti, F. Rapuano, and M. Talevi, Nucl. Phys. B **540** (1999) 472.
- [16] L. Giusti, C. Hoelbling, and C. Rebbi, Phys. Rev. **D 64** (2001) 114508; Erratum, Phys. Rev. **D 65** (2002) 079903.
- [17] P. Hernández, K. Jansen, L. Lellouch, and H. Witting, J. High Energy Phys. **07** (2001) 018; J. Wennekens and H. Witting, J. High Energy Phys. **09** (2005) 059.
- [18] M. Gell-Mann, R. J. Oakes, and B. Renner, Phys. Rev. **175** (1968) 2195; M. Knecht, B. Moussallama, J. Sterna, and H. Fuchs, Nucl. Phys. B **457** (1995) 513; H. Leutwyler, ArXiv:hep-lat/9406283.
- [19] J. Gasser and H. Leutwyler, Phys. Rep. **87** (1982) 77; H. Leutwyler, Phys. Lett. B **378** (1996) 313.
- [20] C. R. Allton, V. Giménez, L. Giusti, F. Rapuano, Nucl. Phys. B **489** (1997) 427.